THE PROTEIN SOCIETY

Cryo-EM structure of fatty acid synthase (FAS) from *Rhodosporidium toruloides* provides insights into the evolutionary development of fungal FAS

Manuel Fischer,[1] Daniel Rhinow,[2] Zhiwei Zhu,[3] Deryck J. Mills,[2] Zongbao K. Zhao,[3,4] Janet Vonck,[2] and Martin Grininger[1]*

[1]Institute of Organic Chemistry and Chemical Biology, Buchmann Institute for Molecular Life Sciences, Cluster of Excellence for Macromolecular Complexes, Goethe University Frankfurt, 60438 Frankfurt am Main, Germany

[2]Department of Structural Biology, Max-Planck-Institute of Biophysics, 60438 Frankfurt, Germany

[3]Division of Biotechnology, Dalian Institute of Chemical Physics, CAS, Dalian 116023, China

[4]Dalian National Laboratory for Clean Energy, Dalian Institute of Chemical Physics, CAS, Dalian 116023, China

Received 15 January 2015; Accepted 2 March 2015
DOI: 10.1002/pro.2678
Published online 2 April 2015 proteinscience.org

Abstract: Fungal fatty acid synthases Type I (FAS I) are up to 2.7 MDa large molecular machines composed of large multifunctional polypeptides. Half of the amino acids in fungal FAS I are involved in structural elements that are responsible for scaffolding the elaborate barrel-shaped architecture and turning fungal FAS I into highly efficient *de novo* producers of fatty acids. *Rhodosporidium toruloides* is an oleaginous fungal species and renowned for its robust conversion of carbohydrates into lipids to over 70% of its dry cell weight. Here, we use cryo-EM to determine a 7.8-Å reconstruction of its FAS I that reveals unexpected features; its novel form of splitting the multifunctional polypeptide chain into the two subunits α and β, and its duplicated ACP domains. We show that the specific distribution into α and β occurs by splitting at one of many possible sites that can be accepted by fungal FAS I. While, therefore, the specific distribution in α and β chains in *R. toruloides* FAS I is not correlated to increased protein activities, we also show that the duplication of ACP is an evolutionary late event and argue that duplication is beneficial for the lipid overproduction phenotype.

Keywords: mega-enzyme; multifunctional proteins; protein assembly; acyl carrier protein; biofuel

Abbreviations: ACP, acyl carrier protein; AT, acetyl transferase; DH, dehydratase; ER, enoyl reductase; FAS I, fatty acid synthase Type I; KR, ketoacyl reductase; KS, ketoacyl synthase; MPT, malonyl-palmitoyl transferase; PPT, phosphopantetheine transferase.

Additional Supporting Information may be found in the online version of this article.

The electron microscopy map has been deposited to the electron microscopy database (EMD) with EMD-6288.

Manuel Fischer purified and analyzed the protein, and wrote the article. Daniel Rhinow performed cryo-EM and processed the data. Zhiwei Zhu established and performed protein purification. Deryck J. Mills performed cryo-EM. Zongbao K. Zhao designed research. Janet Vonck processed and analyzed the data. Martin Grininger analyzed the data, designed the research, and wrote the article

Grant sponsor: German Research Foundation (DFG); Grant number: GR3854 (to M.G.); Grant sponsor: Cluster of Excellence Frankfurt (CEF) "Macromolecular complexes" at the Goethe University Frankfurt (CEF Adjunct Investigatorship Program); Grant sponsor: National Natural Science Foundation of China.; Grant number: 21325627; Grant sponsor: Volkswagen Foundation (Lichtenberg Professorship to M.G. for Research on FAS).

*Correspondence to: Martin Grininger, Institute of Organic Chemistry and Chemical Biology, Buchmann Institute for Molecular Life Sciences, Cluster of Excellence for Macromolecular Complexes, Goethe University Frankfurt, Max-von-Laue-Str. 15, 60438 Frankfurt am Main, Germany. E-mail: grininger@chemie.uni-frankfurt.de

Introduction

Fatty acid synthases Type I (FAS I) are responsible for *de novo* fatty acid synthesis in eukaryotes and CMN group bacteria (*Corynebacterium*, *Mycobacterium*, and *Nocardia*). FAS I occur in MDa-sized assemblies of elaborate architecture in which fatty acids are synthesized in a machine-like fashion. FAS I are made-up of multifunctional polypeptide chains, and distinct from the "conventional" Type II FAS, which are present in most bacteria and mitochondria and provide the catalytic functions for fatty acid synthesis on separate proteins.[1–3]

FAS I can be classified in metazoan and microbial (fungal and bacterial). Metazoan FAS I occur as dimeric complexes of about 0.5 MDa.[4] Current structural progress in the characterization of polyketide synthases Type I (PKS I) strongly suggests that the metazoan FAS I protein fold is widely distributed as an architectural blueprint in the PKS family.[4–8] Microbial FAS I forms multi-oligomeric complexes of sizes between 1.9 MDa (bacterial FAS I) and 2.7 MDa (fungal). The best studied representative of microbial FAS I is the *Saccharomyces cerevisiae* FAS I. It has been extensively analyzed during several decades; for example, its characterization was largely responsible for awarding the Nobel prize to Lynen 50 years ago (1964, awarded jointly to Konrad Bloch and Feodor Lynen for their discoveries in cholesterol and fatty acid metabolism).[9] *S. cerevisiae* FAS I (and *Thermomyces lanuginosus* FAS I) has also been recently analyzed by X-ray crystallography (Fig. 1),[10–13] and the wealth of available functional data have been correlated to structural data, leading to a superior understanding of fungal Type I fatty acid synthesis.[14] For an overview of the catalytic cycle of fatty acid synthesis as performed by fungal FAS I see Supporting Information Fig. S1.

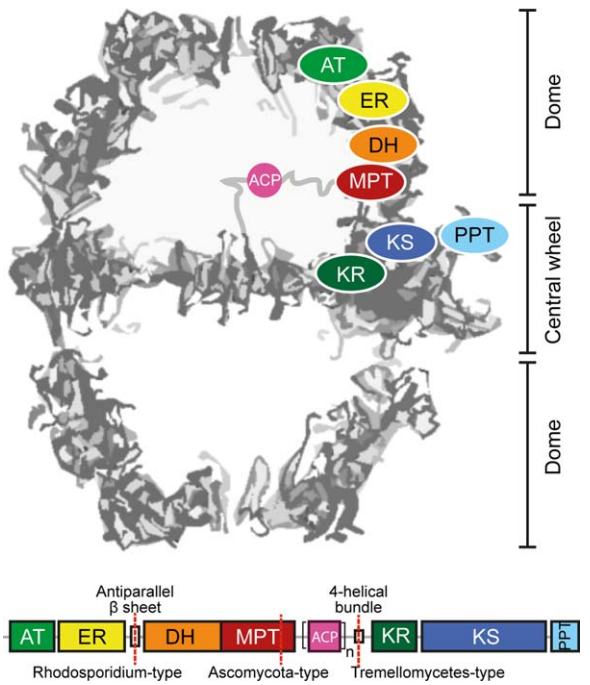

Figure 1. Architecture and domain organization of fungal FAS I. Fungal FAS I is an overall D3 symmetric barrel-shaped complex of homohexameric or heterodocameric ($\alpha_6\beta_6$) oligomerization. For clarity of the structure representation, the protein is abstracted as a cross-section along the threefold axis. Fatty acid synthesis proceeds in two compartments, each of which is lined by three full sets of catalytic domains. The positioning of a set of domains is indicated for the upper compartment. The domains ketoacyl synthase (KS), ketoacyl reductase (KR), and phosphopantetheine transferase (PPT) comprise the central wheel part, while the other domains, acetyl-transferase (AT), enoyl reductase (ER), dehydratase (DH), and malonyl-palmitoyl-transferase (MPT) make up the dome-like structure. Fungal FAS I can be encoded by a single gene, as in the case of the group of *Ustilaginomcetes*, or split into two separate genes (*FAS1* encoding the β-chain and *FAS2* encoding the α-chain) as indicated. A mobile acyl carrier protein (ACP) as a single ($n = 1$) or duplicated domain ($n = 2$) spans the inner volume of the compartments, tethered by flexible linkers to the center of the wheel and the wall of the dome (abstracted by gray lines).

Acyl carrier protein (ACP)-mediated substrate shuttling is a key characteristic of fatty acid synthesis.[3,15] ACP is a small globular protein that after post-translational modification by phosphopantetheine transferases (PPT) is able to bind substrates and intermediates via thioester formation.[16] In Type I systems, ACP is part of the polypeptide chain and in fungal and bacterial FAS I located inside compartmented reaction chambers, where it delivers substrates and intermediates to the active sites of the different enzymatic domains[17,18] (see Fig. 1). A peculiar structural feature that was observed in fungal FAS I is the positioning of the PPT (part of the polypeptide chain in fungal FAS I) at the perimeter of the central wheel.[12] The spatial separation of PPT at the outside of the barrel from ACP in the inside has dramatic consequences for the assembly of the fungal FAS I: The post-translational activation of the ACP domain is not possible in the assembled barrel-like state, but requires an architecturally distinct preassembled state.[12,14,19]

We have started the biochemical and structural characterization of the *Rhodosporidium toruloides* FAS I because of our interest in the evolution and the assembly of FAS I. As a major event in the development of fungal FAS, single gene-encoding FAS split into two gene-encoding (*FAS1* and *FAS2*) variants at different sites (see Fig. 1).[11,14,20] In this light, *R. toruloides* FAS I is a topologically interesting fungal FAS I.[21] It is composed of α- (*FAS2* encoded) and β-chain (*FAS1*) with the splitting site within a β-sheet domain that connects the domains ER and the DH, representing a rare fungal FAS I variant. Further, it shows a duplicated ACP domain, which might correlate to the high oleagenic capacity of the organism. Here, we present the functional and cryo-EM structural characterization of *R.*

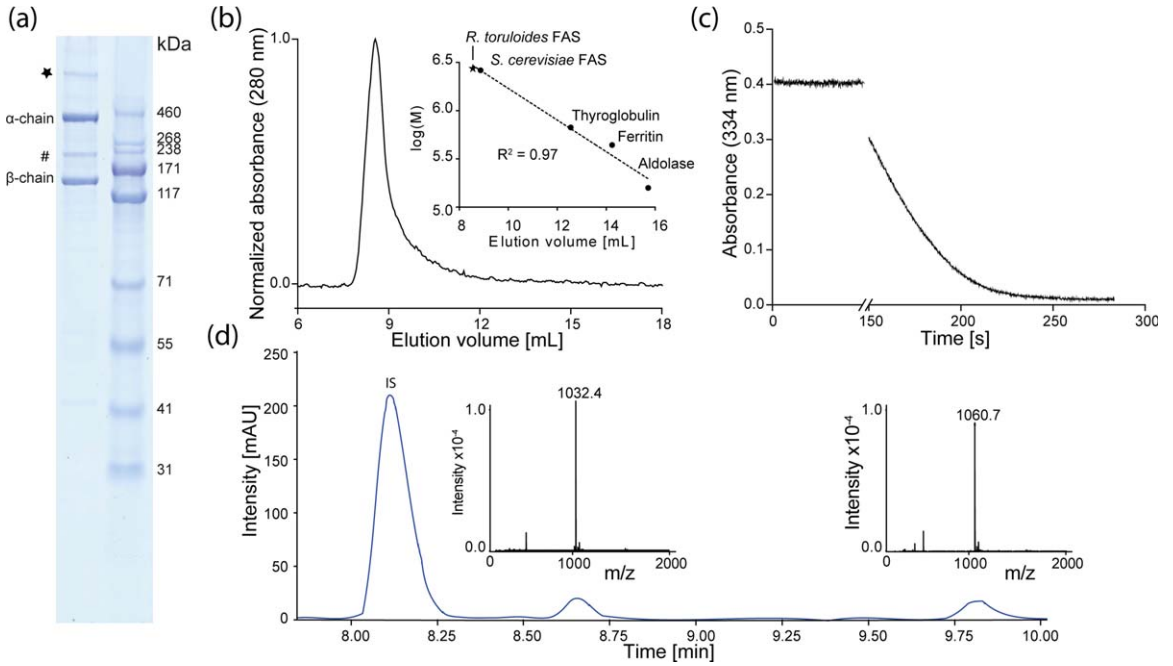

Figure 2. Purification and enzymatic properties of *R. toruloides* FAS I. (a) SDS-PAGE (NuPage Bis-Tris 4–12%, Life Technologies, USA) of purified recombinant FAS I with β-chain (138 kDa) and α-chain (321). A band at about 200 kDa (#) and a band at an apparent molecular weight clearly larger than 500 kDa (*) reflect main impurities. (b) Absorption profile from size exclusion chromatography of *R. toruloides* FAS I on a Superose 6 10/300 column (GE Healthcare). Linear regression of calibration with standard proteins and *S. cerevisiae* FAS I is shown in inset. (c) Absorption profile from activity assay of *R. toruloides* FAS I. Activity at 25°C was monitored by decrease in absorption at 334 nm from consumption of NADPH. (d) HPLC-MS analysis of the *R. toruloides* FAS I product spectrum. Main products are stearic (m/z = 1032.4) and arachidic acid (m/z = 1060.7); IS, internal standard (isoheptadecanoyl-CoA).

toruloides FAS I. We discuss our data in light of the evolution of fungal FAS I toward the highly efficient molecular machines as they appear in the oleaginous strain *R. toruloides*, and we propose that the assembly of the up to 2.7 MDa large protein complexes is a robust sequential process, running through a defined sequence of events.

Results

Recombinant expression of R. toruloides FAS I

Fully assembled and functional wild-type *R. toruloides* FAS I was successfully expressed in *Escherichia coli* at a yield of more than 6 mg per liter culture. The FAS I complex was purified via a multi-step purification protocol [Fig. 2(A)]. Final size exclusion chromatography shows a monodisperse UV-absorption peak at an apparent molecular weight of about 2.7 MDa representing the $\alpha_6\beta_6$ heterododecameric complex [Fig. 2(B)]. Tailing of the high oligomeric peak indicates minor impurities or protein degradation, as also observable in SDS-PAGE. In SDS-PAGE, a faint band was observed appearing with a higher apparent molecular weight than 460 kDa, which we speculated to occur from stable interactions of α- and β-chain to a higher oligomeric species that does not dissociate during sample preparation. However, variations in the strength of the denaturing conditions did not lead to varying band intensities [see Fig. 2(A)].

Enzymatic analysis

The enzymatic activity of *R. toruloides* FAS I was tested by monitoring NADPH consumption via absorption at 334 nm [Fig. 2(C)]. As an average of three independent protein preparations, we obtained a specific activity of 476 ± 159 mU/mg with respect to the consumption of two equivalents NADPH per reaction, reflecting one reaction cycle and the elongation of the fatty acid by one C_2-unit. The individual protein batches showed specific activities of 618 ± 132 mU/mg, 506 ± 85 mU/mg and 304 ± 31 mU/mg, respectively. *S. cerevisiae* FAS I from native preparations yielded activities ranging from 343 mU/mg[22] to 3500 mU/mg.[23,24] Considering the particular architecture of the duplicated ACP as a means for increasing the capacity of substrate shuttling, *R. toruloides* FAS I activity is lower than expected. Negative stain EM, initially performed for monitoring protein quality, and cryo-EM show high protein homogeneity. It is tempting to speculate that low protein activities might reflect incomplete post-translational phosphopantetheinylation as a consequence of the heterogeneous environment during recombinant expressions. Alternatively, it might be resulted from insufficient cofactor (FMN) binding or

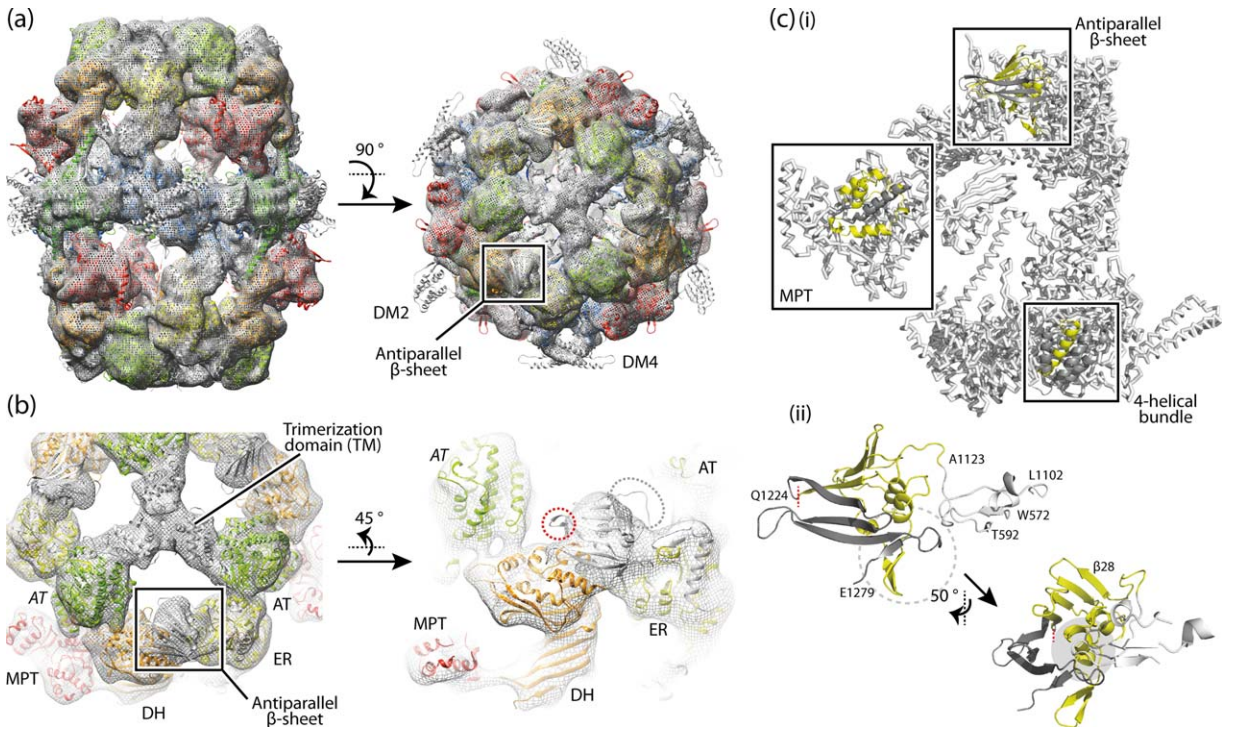

Figure 3. The structure of *R. toruloides* FAS I. (a) Cryo-EM map at 7.8 Å resolution with the X-ray structure of *T. lanuginosus* FAS I (pdb codes 2uva, 2uvb)[11] fitted into the map as a rigid body. The protein is shown in side and top view. The polypeptides are colored according to the scheme above (see Fig. 1). Structural elements and the antiparallel β-sheet are highlighted. (b) 3D map and structural model as in (a) with zoom onto the antiparallel β-sheet domain. Domains are labeled. *AT* (italic letters) is provided from the neighboring polypeptide chain. The splitting site as occurring in *R. toruloides* FAS I is highlighted by a red circle; the loop connecting the β-sheet with the ER by a gray circle. (c, i) A single α-chain and a single β-chain are extracted from the fungal FAS I (*T. lanuginosus* FAS I; pdb codes 2uva, 2uvb)[11] and splitting sites as occurring in fungal FAS I types *Ascomycota* (splitting site within MPT domain), *Tremellomycetes* (splitting site within 4-helical bundle) and *Rhodosporidium* (splitting site within antiparallel β-sheet) are indicated. In the highlighted structural elements, the β-chain part is shown in yellow and the α-chain part in dark gray. (ii) Antiparallel β-sheet composed of the β-chain and α-chain of *R. toruloides* FAS I; model and coloring as in (i); the left figure is roughly in the orientation of the side view in (a). The interface is comprised by formation of a curved β-sheet that interacts with α-helices at the concave face (highlighted by gray background), intertwined hairpin loops (highlighted by dashed circle), and the hairpin loop of α-chain interacting with a globular fold of the ER domain (colored in white). Residue numbers are given for defining borders (*T. lanuginosus* FAS I numbering).

the presence of protein tags. We also analyzed the product spectrum of *R. toruloides* FAS I by HPLC-MS, and detected C_{18}- and C_{20}-acyl CoA esters as the main products [Fig. 2(D)]. This is different to reported data, showing exclusively production of C_{16}- and C_{18}-fatty acids *in vivo*,[25–27] and might reflect the difference between *in vitro* assay conditions and the *in vivo* environment; for example, different relative levels of malonyl- and acetyl-CoA concentrations[28] or interfering macromolecules.[29,30]

Three-dimensional cryo-EM map

We generated a 3D map of *R. toruloides* FAS I from 3296 particles (Supporting Information Fig. S2). The resolution of the final map was measured by the Fourier shell correlation (FSC) method at the FSC 0.143 criterion as 7.8 Å.[31] The map resolves all features of fungal FAS I that were seen before in X-ray[11–13,18] and cryo-EM studies[17] [Fig. 3(A)]. Docking of available structural information revealed that the map is more similar to published X-ray structures of *T. lanuginosus* and *S. cerevisiae* FAS I than to the cryo-EM structure of *S. cerevisiae* FAS I. In the *S. cerevisiae* FAS I cryo-EM structure,[17] differences in domain positions were observed that lead to overall shorter (by ~20 Å) but wider (by ~18 Å) barrel-like structure. Most significant was a ~9° rotated arrangement of the trimerization domains (TM) at the threefold axis.[17] Our data revise the initial assumption that the X-ray structures of yeast FAS I might have been affected by crystal contacts, but suggest a breathing-like motion as real conformational variability of fungal FAS I. Unlike the *S. cerevisiae* FAS I cryo-EM map, the *R. toruloides* map showed no evidence of heterogeneity (Supporting Information Fig. S3), which characterizes the *R. toruloides* FAS I barrel as rigid which is in line with previous data.[1,14] Density for the ACP domains was not visible in the map, indicating that they occupy varying positions inside the reaction chambers.

By carrying the gene splitting site within the β-sheet domain encoding sequence, *R. toruloides*

FAS I of the *Sporidiobolales* clade represents a specific case of two gene-encoding fungal FAS I variant. Docking of the *T. lanuginosus* FAS I X-ray structure into the EM map supports sequence analysis (Supporting Information Fig. S4) and does not reveal any unexpected features [Fig. 3(A,B)]. The loop connecting the antiparallel β-sheet with the ER and the loop carrying the splitting site protrude from the electron density [Fig. 3(B)]. These properties might be due to minor local structural differences between *R. toruloides* FAS I (map) and *T. lanuginosus* FAS I (model), or to local conformational variability, which cannot be traced at this resolution. Here it is worth to mention that also in the 3.1 Å X-ray structure the connecting linker as well as the first β-strand of the antiparallel β-sheet (β28) could not be traced in electron density (K1122-N1140, corresponding *T. lanuginosus* FAS I numbering).[18]

Discussion

We have recently started the structural and functional characterization of *R. toruloides* FAS I from recombinant expressions in *E. coli* because of our interest in the evolutionary development of fungal FAS I. *R. toruloides* is a high lipid producing fungal species, and initial characterizations speculated on *R. toruloides* encoding FAS I with improved fatty acid productivity.[21]

In *R. toruloides* FAS I, we were particularly interested in the novel form of splitting the multifunctional polypeptide into a β-chain which solely carries the domains AT and ER, and in an α-chain which includes all other domains. As expected, our data do not reveal any features emerging from the domain distribution that might be correlated with increased protein activity. Interestingly, the interaction of the α- and β-chain is different as compared to the other topical variants. In *S. cerevisiae* and *T. lanuginosus* FAS I, both representing the *Ascomycota* fungal FAS I variant, the α- and β-chain interact via termini that intertwine in forming a helical bundle as part of the MPT domain [Fig. 3(C)].[11,18] From homology modeling with available structural information, it can be assumed that also FAS of the *Tremellomycetes* variant share the characteristic of chains interacting via intertwined termini. Here, the C-terminus of the β-chain and the N-terminus of the α-chain form a 4-helical bundle in the interface of the KR and the KS domain [Fig. 3(C)]. The interaction of chains in *R. toruloides* FAS I is conceptually different. Similar to the *Ascomycota* and the *Tremellomycetes* variants, the polypeptide chains interact within a domain (β-sheet domain, L1102-E1279, *T. lanuginosus* numbering). However, rather than showing intertwined termini, a large interface of 1725 Å^2 (PDB ID: 2uva; *T. lanuginosus*)[11] is formed [Fig. 3(C)]. Cryo-EM data are clearly at too low resolution to trace details of the interaction of the polypeptide chains, but the smooth incorporation of the *T. lanuginosus* FAS I structural model into *R. toruloides* FAS I cryo-EM density [see Fig. 3(A,B)] implies that there are no substantial differences in the fold of the ER-DH connecting β-sheet domain, in line with alignments and secondary structure predictions (see Supporting Information Fig. S4).

Gene splitting in two gene-encoded variants is an evolutionary late event,[14,32] and the topological variants currently identified from available sequence information are relevant for understanding the assembly of fungal FAS I. Recently, the idea of the evolutionary conservation of assembly pathways has been established.[33] For fungal FAS I, evolutionary pressure for the conservation of the assembly pathway arises from the structural particularity of the spatially separated domains ACP and PPT in the mature barrel-like structure. As they are hindered in forming productive interactions in the mature structure, the phosphopantetheinylation of ACP by PPT has to occur in a preassembled state.[12,19] From the common motif of the interactions of chains within domains, we speculate that in the process of assembly, the two gene-encoding variants form pseudo-single chains so that all variants align into a single pathway in an early step. Subsequently, these initial assemblies arrange into the preassembled states competent for post-translational modification of ACP. From the structural appearance of the interaction of chains in two gene-encoded fungal FAS I, it is tempting to speculate that the assembly pathway of fungal FAS I is a robust sequential process, that putatively accepts many splitting sites, as long as the interactions of the polypeptide chains is strong enough, either by intertwining termini, as observed in *Ascomycota* and the *Tremellomycetes* variants, or by forming large interfaces as observed for the *Rhodosporidium* variant.

Another interesting feature of *R. toruloides* FAS I is the duplication of the ACP domain. As evident from the structural characterization of *R. toruloides* FAS I (see Supporting Information Fig. S3) and reported for *S. cerevisiae* FAS I before,[17,18] the extensive scaffolding in fungal FAS I leads to conformationally restricted proteins in which essentially only the substrate shuttling ACP is mobile owing to conformationally variable linkers. The ACP domains are 77% sequence identical and show particular high conservation in regions relevant for docking (Supporting Information Fig. S6). From sequence conservation, a specialization among the two ACP domains for any of the steps relevant for fatty acid synthesis is unlikely. Similar to what was shown for multienzyme proteins in polyunsaturated fatty acid (PUFA) production that carry tandem ACP domains, the purpose of ACP duplication in *R. toruloides* FAS I seems to lie in the increase in its apparent ACP concentration and, consequently, the increase in the

capacity for shuttling substrates and intermediates.[34,35] Additional benefit arises from crowding of the reaction chamber with a second ACP domain and a connecting linker.[36] Our cryo-EM data did not allow assignment of ACP positions, reflecting the positional variability of the ACP as an inherent feature of FAS I systems.[1,17] An interesting aspect is the occurrence of the duplicated ACP across the phylogenetic clades that define the fungal FAS I variants (Supporting Information Fig. S5). This gives evidence that the duplication of ACP is an evolutionary recent development that occurred after the evolutionary event of the splitting of the single gene-encoded fungal FAS I in the currently known two gene-encoded variants.

Conclusion

FAS I are among the most complex proteins analyzed in eukaryotes.[1,14] They are made up of multifunctional polypeptides that assemble to up to 2.7 MDa large complexes of elaborate architecture. Fungal FAS I are highly evolved. Their development comprises hallmarks as follows: (i) The extension of individual monofunctional proteins with scaffolding domains.[32] (ii) Fusion events of the monofunctional proteins to a stable single gene-encoded multifunctional FAS I protein.[32] This FAS I ancestor protein is distributed in *Corynebacteria*, *Mycobacteria*, and *Nocardia*. (iii) Further scaffolding to a single gene-encoded fungal FAS I.[20,37] (iv) Gene splitting into two gene-encoded variants. Many splitting sites may be tolerated as long as they do not interfere in FAS I assembly. (v) ACP duplication in certain species, as *R. toruloides* FAS I, for increasing the substrate shuttling capacity.

Material and Methods

Plasmid construction

Total RNA was prepared as described previously.[21] cDNA synthesis was performed with PrimeScript High Fidelity RT-PCR Kit (Takara, Dalian, China). FAS coding genes were amplified with primer pairs (FAS1-5-NdeI, GGCATTCCATATGGCAAGCTGGAGCCACCCGCAGTTCGAAAAGGGTGCAATGAACGGCCGAGCGACGCG, FAS1-3-EcoRI, GGAATTCTCAGAGCCCGCCGAAGACG, FAS2-5-HindIII, GCCCAAGCTTATGGTCGCGGCGCAGGACTTG and FAS2-3-NotI, CCGCATTGCGGCCGCCTTCTGGGCGATGACGACGGC). The β-chain encoding fragment inserted into pET22b(+) vector (Novagen, Darmstadt, Germany) yielded pET22b-*Rt*FAS1, while the α-chain fragment inserted into pET24b(+) vector (Novagen, Darmstadt, Germany) gave pET24b-*Rt*FAS2-WT. Plasmids were coding for a β-chain carrying an N terminal Strep-II-tag (MASWSHPQFEKGA-), and the α-chain modified with an N terminal T7-tag (MASMTGGQQMGRDPNSSSVDKL-) and a C terminal His_6-tag (-AAALEHHHHHH).

Recombinant expression and purification of Rhodosporidium FAS

E. coli strain BL21 (DE3; Novagen, Darmstadt, Germany) was co-transformed with plasmids pET22b-*Rt*FAS1 and pET24b-*Rt*FAS2-WT via the heat shock method and selected on LB agar supplemented with an appropriate amount of antibiotics (100 μg/mL ampicillin and 50 μg/mL kanamycin). Expression and purification of the recombinant *Rhodosporidium* FAS I was described before.[38] Briefly, single colonies were used to inoculate 5 mL of a LB preculture, which finally was used to inoculate 1.6 L TB media (with 100 μg/mL ampicillin and 50 μg/mL kanamycin). After growth to OD_{600} of 0.6–0.8, the expression was induced by adding IPTG to the medium to a final concentration of 0.5 m*M*. The culture was incubated at 200 rpm and 16°C for 30 h. Cells were harvested by centrifugation at 8000 rpm (6200*g*) for 10 min. The cell pellet (about 12 g) was resuspended in 36 mL lysis buffer (100 m*M* KPi pH 7.0, 5 m*M* EDTA, 5 m*M* β-mercaptoethanol, 1 m*M* phenylmethylsulfonylfluoride, 3 m*M* $MgCl_2$, 0.5 mg/mL lysozyme (Genview, Beijing, China), protease inhibitor tablets (Roche, Basel, Switzerland) and homogenized by ultrasonication for 20 min. The lysate was cleared by centrifugation at 14,000 rpm (18,000*g*) for 30 min. Saturated $(NH_4)_2SO_4$ solution was added to the supernatant (25%, v/v), and the mixture was stirred for 30 min. Precipitated protein was pelleted at 14,000 rpm (18,000*g*) for 30 min. A second protein pellet was obtained in a similar protocol, adding additional saturated $(NH_4)_2SO_4$ solution to 33% (v/v). Pellets were resuspended in 16 mL buffer A (20 m*M* HEPES pH 8.0, 100 m*M* KCl, 5 m*M* EDTA, 5 m*M* β-mercaptoethanol), and loaded onto a 10–40% (w/v) sucrose density gradient (in buffer A). The centrifugation was performed in a SW32 rotor at 27,000 rpm (about 90,000*g*) and 4°C for 15 h. FAS I containing fractions were collected and ultrafiltrated. Subsequently, anion exchange chromatography (DEAE-sepharose) was performed. Proteins were eluted with KCl by gradients of buffer A and B (20 m*M* HEPES pH 8.0, 800 m*M* KCl, 5 m*M* EDTA, 5 m*M* β-mercaptoethanol). FAS I containing fractions were concentrated and a second run of sucrose density centrifugation was performed for further purification. More than 10 mg protein was obtained.

Size exclusion chromatography

Size exclusion chromatography was performed on a Superose 6 10/300 GL column (GE Healthcare). After equilibration of the column with buffer (100 m*M* sodium phosphate pH 7.2, 200 m*M* NaCl, 1 m*M* EDTA), 500 μL of protein in buffer A (1.4 mg/mL) was loaded onto the column. 1 mL fractions

were collected with a flow rate of 0.3 mL/min, and absorption at 280 nm was recorded. During all steps, the protein was always kept at 4°C. The calibration of the chromatographic system was done with a high molecular weight gel filtration calibration kit (GE Healthcare).

Enzymatic activity assay

Enzyme activity was determined by recording the NADPH-consumption via the decrease in absorption at 334 nm in an UV/vis-spectrometer (Lambda 25; Perkin Elmer). The assay was performed with 25 μg protein in a buffered solution (200 m*M* potassium phosphate pH 7.3, 87.5 μ*M* DTT, 250 m*M* NADPH, 417 m*M* acetyl-CoA, 500 m*M* malonyl-CoA) with a total volume of 120 μL at room temperature. The activity analysis comprises only the linear range of the absorption curve after malonyl-CoA-addition. One unit of FAS I activity is defined as the turnover of 1 μmol malonyl-CoA or 2 μmol NADPH per minute, respectively.

Enzymatic product spectrum

To analyze the product spectrum of *R. toruloides* FAS I, the enzymatic reaction was performed in buffered solution (200 m*M* potassium phosphate pH = 7.3, 87.5 μ*M* DTT, 2.25 m*M* NADPH, 0.20 m*M* acetyl-CoA, 1.00 m*M* malonyl-CoA) with a total volume of 100 μL and with 20 μg of protein. The reaction was kept at room temperature for 18 h and stopped by freezing the samples in liquid nitrogen. Work-up was done by acetone precipitation of the protein and vacuum evaporation of the solvent. The residue was redissolved in 50 μL water and analyzed by HPLC-MS.

Cryo-EM data collection

A 1.3-mg/mL FAS I sample of 3 μL was applied to glow discharged Quantifoil R2/2 holey carbon grids (Quantifoil Micro Tools, Jena, Germany). The samples were vitrified using an FEI Vitrobot plunge-freezer. Data was collected on an FEI Tecnai Polara operating at 300 kV, using a back-thinned FEI Falcon II direct electron detector. The Falcon II camera was calibrated at the desired nominal magnification of 78,000×. The calibrated magnification on the 14 μm pixel camera was 106,000×, resulting in a 1.32 Å pixel size at the specimen. The camera system was set up to record 18 frames/s.[39,40] Videos were collected for 1.5 s with a total of 24 frames with a calibrated dose of 3.5e^{-}/Å^2 per frame, at defocus values of 1.5–3 μm.

Image processing

The 24 frames of each video were aligned using the whole-image motion correction method described in Li *et al.*[41] Particle picking was carried out using the manual procedure of EMAN Boxer,[42] and the contrast transfer function of every image was determined using CTFFIND3[43] in the RELION workflow.[44] The data set was refined with the gold standard refinement procedure of RELION,[45] using the cryo-EM map of *S. cerevisiae* FAS I[17] low-pass filtered to 60 Å as a starting model, using 20 frames (from frame 2 to frame 21). A postprocessing procedure implemented in RELION[44] was applied to the final maps for appropriate masking, B-factor sharpening and resolution validation.[46] The final map of 3296 particles has a resolution of 7.8 Å by the FSC 0.143 criterion[31] after applying this postprocessing procedure. The local resolution of the map was estimated with the Resmap software (available at http://resmap.sourceforge.net).[47] The map was displayed in USCF Chimera,[48] and the structure of *T. lanuginosus* FAS I (pdb codes 2uva, 2uvb)[11] was fitted into the map as a rigid body without further refinement.

Acknowledgment

We are grateful to Werner Kühlbrandt for his continuous support of our research focus on the structural characterization of FAS mega-enzymes.

References

1. Maier T, Leibundgut M, Boehringer D, Ban N (2010) Structure and function of eukaryotic fatty acid synthases. Q Rev Biophys 43:373–422.
2. Gago G, Diacovich L, Arabolaza A, Tsai SC, Gramajo H (2011) Fatty acid biosynthesis in actinomycetes. FEMS Microbiol Rev 35:475–497.
3. Schweizer E, Hofmann J (2004) Microbial type I fatty acid synthases (FAS): major players in a network of cellular FAS systems. Microbiol Mol Biol Rev 68:501–517.
4. Maier T, Leibundgut M, Ban N (2008) The crystal structure of a mammalian fatty acid synthase. Science 321:1315–1322.
5. Keatinge-Clay AT (2012) The structures of type I polyketide synthases. Nat Prod Rep 29:1050–1073.
6. Dutta S, Whicher JR, Hansen DA, Hale WA, Chemler JA, Congdon GR, Narayan AR, Håkansson K, Sherman DH, Smith JL, Skiniotis G (2014) Structure of a modular polyketide synthase. Nature 510:512–517.
7. Edwards AL, Matsui T, Weiss TM, Khosla C (2014) Architectures of whole-module and bimodular proteins from the 6-deoxyerythronolide B synthase. J Mol Biol 426:2229–2245.
8. Rittner A, Grininger M (2014) Modular polyketide synthases (PKSs): a new model fits all? Chembiochem 15: 2489–2493.
9. Lynen F (1965) From "activated acetic acid" to terpenes and fatty acids. Umsch Wiss Tech 65:321–326.
10. Jenni S, Leibundgut M, Maier T, Ban N (2006) Architecture of a fungal fatty acid synthase at 5 Å resolution. Science 311:1263–1267.
11. Jenni S, Leibundgut M, Boehringer D, Frick C, Mikolasek B, Ban N (2007) Structure of fungal fatty acid synthase and implications for iterative substrate shuttling. Science 316:254–261.

12. Lomakin IB, Xiong Y, Steitz TA (2007) The crystal structure of yeast fatty acid synthase, a cellular machine with eight active sites working together. Cell 129:319–332.
13. Johansson P, Wiltschi B, Kumari P, Kessler B, Vonrhein C, Vonck J, Oesterhelt D, Grininger M (2008) Inhibition of the fungal fatty acid synthase type I multienzyme complex. Proc Natl Acad Sci U S A 105: 12803–12808.
14. Grininger M (2014) Perspectives on the evolution, assembly and conformational dynamics of fatty acid synthase type I (FAS I) systems. Curr Opin Struct Biol 25:49–56.
15. White SW, Zheng J, Zhang Y-M, Rock CO (2005) The structural biology of type II fatty acid biosynthesis. Annu Rev Biochem 74:791–831.
16. Beld J, Sonnenschein EC, Vickery CR, Noel JP, Burkart MD (2014) The phosphopantetheinyl transferases: catalysis of a post-translational modification crucial for life. Nat Prod Rep 31:61–108.
17. Gipson P, Mills DJ, Wouts R, Grininger M, Vonck J, Kuhlbrandt W (2010) Direct structural insight into the substrate-shuttling mechanism of yeast fatty acid synthase by electron cryomicroscopy. Proc Natl Acad Sci USA 107:9164–9169.
18. Leibundgut M, Jenni S, Frick C, Ban N (2007) Structural basis for substrate delivery by acyl carrier protein in the yeast fatty acid synthase. Science 316:288–290.
19. Johansson P, Mulinacci B, Koestler C, Vollrath R, Oesterhelt D, Grininger M (2009) Multimeric options for the auto-activation of the *Saccharomyces cerevisiae* FAS type I megasynthase. Structure 17:1063–1074.
20. Boehringer D, Ban N, Leibundgut M (2013) 7.5-Å cryo-em structure of the mycobacterial fatty acid synthase. J Mol Biol 425:841–849.
21. Zhu Z, Zhang S, Liu H, Shen H, Lin X, Yang F, Zhou YJ, Jin G, Ye M, Zou H, Zhao ZK (2012) A multi-omic map of the lipid-producing yeast *Rhodosporidium toruloides*. Nat Commun 3:1112.
22. Morisaki N, Funabashi H, Shimazawa R, Furukawa J, Kawaguchi A, Okuda S, Iwasaki S (1993) Effect of side-chain structure on inhibition of yeast fatty-acid synthase by cerulenin analogs. Eur J Biochem 211: 111–115.
23. Fichtlscherer F, Wellein C, Mittag M, Schweizer E (2000) A novel function of yeast fatty acid synthase. Subunit alpha is capable of self-pantetheinylation. Eur J Biochem/FEBS 267:2666–2671.
24. Wieland F, Renner L, Verfürth C, Lynen F (1979) Studies on the multi-enzyme complex of yeast fatty-acid synthetase. Eur J Biochem 94:189–197.
25. Davoli P, Mierau V, Weber RWS (2004) Carotenoids and fatty acids in red yeasts Sporobolomyces roseus and Rhodotorula glutinis. Appl Biochem Microbiol 40: 392–397.
26. Easterling ER, French WT, Hernandez R, Licha M (2009) The effect of glycerol as a sole and secondary substrate on the growth and fatty acid composition of Rhodotorula glutinis. Bioresource Technol 100:356–361.
27. Xu J, Zhao X, Wang W, Du W, Liu D (2012) Microbial conversion of biodiesel byproduct glycerol to triacylglycerols by oleaginous yeast *Rhodosporidium toruloides* and the individual effect of some impurities on lipid production. Biochem Eng J 65:30–36.
28. Sumper M, Oesterhelt D, Riepertinger C, Lynen F (1969) Synthesis of various carboxylic acids by the multienzyme complex of fatty acid synthesis from yeast, and clarification of their structure. Eur J Biochem/FEBS 10:377–387.
29. Peterson DO, Bloch K (1977) Mycobacterium smegmatis fatty acid synthetase. Long chain transacylase chain length specificity. J Biol Chem 252: 5735–5739.
30. Zimhony O, Vilcheze C, Jacobs WR, Jr. (2004) Characterization of Mycobacterium smegmatis expressing the Mycobacterium tuberculosis fatty acid synthase I (fas1) gene. J Bacteriol 186:4051–4055.
31. Rosenthal PB, Henderson R (2003) Optimal determination of particle orientation, absolute hand, and contrast loss in single-particle electron cryomicroscopy. J Mol Biol 333:721–745.
32. Bukhari HST, Jakob RP, Maier T (2014) Evolutionary origins of the multienzyme architecture of giant fungal fatty acid synthase. Structure 22: 1775–1785.
33. Marsh JA, Hernández H, Hall Z, Ahnert SE, Perica T, Robinson CV, Teichmann SA (2013) Protein complexes are under evolutionary selection to assemble via ordered pathways. Cell 153:461–470.
34. Jiang H, Zirkle R, Metz JG, Braun L, Richter L, Van Lanen SG, Shen B (2008) The role of tandem acyl carrier protein domains in polyunsaturated fatty acid biosynthesis. J Am Chem Soc 130:6336–6337.
35. Trujillo U, Vázquez-Rosa E, Oyola-Robles D, Stagg LJ, Vassallo DA, Vega IE, Arold ST, Baerga-Ortiz A (2013) Solution structure of the tandem acyl carrier protein domains from a polyunsaturated fatty acid synthase reveals beads-on-a-string configuration. PLoS One 8: e57859. .
36. Anselmi C, Grininger M, Gipson P, Faraldo-Gomez J (2010) Mechanism of substrate shuttling by the acyl-carrier protein within the fatty acid mega-synthase. J Am Chem Soc 132:12357–12364.
37. Ciccarelli L, Connell SR, Enderle M, Mills DJ, Vonck J, Grininger M (2013) Structure and conformational variability of the Mycobacterium tuberculosis fatty acid synthase multienzyme complex. Structure 21:1251–1257.
38. Zhu Z, Zhang S, Lin X, Liu W, Zhao ZK (2014) Expression, purification and characterization of a novel fatty acid synthase from *Rhodosporidium toruloides*. Chin J Biotech 30:1414–1423.
39. Allegretti M, Mills DJ, McMullan G, Kühlbrandt W, Vonck J (2014) Atomic model of the F420-reducing [NiFe] hydrogenase by electron cryomicroscopy using a direct electron detector. eLife 3:e01963.
40. Bai X-c, Fernandez IS, McMullan G, Scheres SHW (2013) Ribosome structures to near-atomic resolution from thirty thousand cryo-EM particles. eLife 2: e00461.
41. Li X, Mooney P, Zheng S, Booth CR, Braunfeld MB, Gubbens S, Agard DA, Cheng Y (2013) Electron counting and beam-induced motion correction enable near-atomic-resolution single-particle cryo-EM. Nat Methods 10:584–590.
42. Ludtke SJ, Baldwin PR, Chiu W (1999) EMAN: semiautomated software for high-resolution single-particle reconstructions. J Struct Biol 128:82–97.
43. Mindell JA, Grigorieff N (2003) Accurate determination of local defocus and specimen tilt in electron microscopy. J Struct Biol 142:334–347.

44. Scheres SH (2012) RELION: implementation of a Bayesian approach to cryo-EM structure determination. J Struct Biol 180:519–530.
45. Scheres SH, Chen S (2012) Prevention of overfitting in cryo-EM structure determination. Nat Methods 9:853–854.
46. Chen S, McMullan G, Faruqi AR, Murshudov GN, Short JM, Scheres SHW, Henderson R (2013) High-resolution noise substitution to measure overfitting and validate resolution in 3D structure determination by single particle electron cryomicroscopy. Ultramicroscopy 135:24–35.
47. Kucukelbir A, Sigworth FJ, Tagare HD (2014) Quantifying the local resolution of cryo-EM density maps. Nat Methods 11:63–65.
48. Pettersen EF, Goddard TD, Huang CC, Couch GS, Greenblatt DM, Meng EC, Ferrin TE (2004) UCSF Chimera—a visualization system for exploratory research and analysis. J Comput Chem 25:1605–1612.